

Sustained translational repression by eIF2 α -P mediates prion neurodegeneration

Julie A. Moreno¹, Helois Radford¹, Diego Peretti¹, Joern R. Steinert¹, Nicholas Verity¹, Maria Guerra Martin¹, Mark Halliday¹, Jason Morgan¹, David Dinsdale¹, Catherine A. Ortori², David A. Barrett², Pavel Tsaytler³, Anne Bertolotti³, Anne E. Willis¹, Martin Bushell¹ & Giovanna R. Mallucci¹

The mechanisms leading to neuronal death in neurodegenerative disease are poorly understood. Many of these disorders, including Alzheimer's, Parkinson's and prion diseases, are associated with the accumulation of misfolded disease-specific proteins. The unfolded protein response is a protective cellular mechanism triggered by rising levels of misfolded proteins. One arm of this pathway results in the transient shutdown of protein translation, through phosphorylation of the α -subunit of eukaryotic translation initiation factor, eIF2. Activation of the unfolded protein response and/or increased eIF2 α -P levels are seen in patients with Alzheimer's, Parkinson's and prion diseases¹⁻⁴, but how this links to neurodegeneration is unknown. Here we show that accumulation of prion protein during prion replication causes persistent translational repression of global protein synthesis by eIF2 α -P, associated with synaptic failure and neuronal loss in prion-diseased mice. Further, we show that promoting translational recovery in hippocampi of prion-infected mice is neuroprotective. Overexpression of GADD34, a specific eIF2 α -P phosphatase, as well as reduction of levels of prion protein by lentivirally mediated RNA interference, reduced eIF2 α -P levels. As a result, both approaches restored vital translation rates during prion disease, rescuing synaptic deficits and neuronal loss, thereby significantly increasing survival. In contrast, salubrinal, an inhibitor of eIF2 α -P dephosphorylation⁵, increased eIF2 α -P levels, exacerbating neurotoxicity and significantly reducing survival in prion-diseased mice. Given the prevalence of protein misfolding and activation of the unfolded protein response in several neurodegenerative diseases, our results suggest that manipulation of common pathways such as translational control, rather than disease-specific approaches, may lead to new therapies preventing synaptic failure and neuronal loss across the spectrum of these disorders.

Neurodegenerative diseases pose an ever-increasing challenge for society and health care systems worldwide, but their molecular pathogenesis is still largely unknown and no curative treatments exist. Alzheimer's (AD), Parkinson's (PD) and prion diseases are separate clinical and pathological conditions, but it is likely they share common mechanisms leading to neuronal death. Mice with prion disease show misfolded prion protein (PrP) accumulation and develop extensive neurodegeneration (with profound neurological deficits), in contrast to mouse models of AD or PD, in which neuronal loss is rare. Uniquely therefore, prion-infected mice allow access to mechanisms linking protein misfolding with neuronal death. Prion replication involves the conversion of cellular PrP, PrP^C, to its misfolded, aggregating conformer, PrP^{Sc}, a process leading ultimately to neurodegeneration⁶. We have previously shown rescue of neuronal loss and reversal of early cognitive and morphological changes in prion-infected mice by depleting PrP in neurons, preventing prion replication and abrogating neurotoxicity⁷⁻⁹. However, the molecular mechanisms underlying both the progression of disease, and those underlying recovery in PrP-depleted animals, were unknown.

To understand these processes better, we now analysed the evolution of neurodegeneration in prion-diseased mice. We examined hippocampi from prion-infected tg37 mice used in our previous experiments⁷⁻¹⁰, in which the time course of impairment and recovery are clearly defined. Hemizygous tg37 mice express mouse PrP at approximately three times wild-type levels and succumb to Rocky Mountain Laboratory (RML) prion infection within 12 weeks post infection (w.p.i.)¹⁰. They first develop behavioural signs with decreased burrowing activity at approximately 9 w.p.i., after reduction in hippocampal synaptic transmission and first neuropathological changes^{7,8}. This is the window of reversibility when diseased neurons can still be rescued: PrP depletion up to 9 w.p.i., but not later, rescues neurotoxicity, as by 10 w.p.i. neuronal loss is established⁷⁻⁹. We measured PrP levels, synapse number, levels of synaptic proteins and synaptic transmission in prion-infected mice weekly from 5 w.p.i., and burrowing behaviour from 6 w.p.i. We examined brains histologically and counted CA1 neurons. (Cohorts of at least 30 animals were used per group; biochemical and histological analyses were done on three mice per time point, burrowing behaviour on 12, *n* for other analyses is indicated in figure legends.) We found an early decline in synapse number in asymptomatic animals at 7 w.p.i. to approximately 55% of control levels (Fig. 1a), despite unchanged levels of several pre- and post-synaptic marker proteins (Fig. 1b). Reduced synapse number with normal synaptic protein levels is likely to reflect impaired structural plasticity of synapses at this early stage of disease. At 9 w.p.i., however, there was a sudden decline in synaptic protein levels to approximately 50% of control levels for several pre- (SNAP-25 and VAMP-2) and postsynaptic (PSD-95 and NMDAR1) proteins (Fig. 1b and Supplementary Fig. 1b). This was associated with further decline in synapse number, and the critical reduction in synaptic transmission, both in amplitude of evoked excitatory postsynaptic currents (EPSCs) and in the number of spontaneous miniature EPSCs (mEPSCs) in CA1 neurons (Fig. 1c and Supplementary Fig. 1e). This was coincident with behavioural change (Fig. 1d) and first spongiform pathology (Supplementary Fig. 1d), and was rapidly followed by the onset of neurodegeneration, resulting in 50% reduction in hippocampal pyramidal neurons at 10 w.p.i. (Fig. 1e). All animals developed overt motor signs and were terminally sick by 12 w.p.i.

The abrupt loss of synaptic proteins at 9 w.p.i. appeared to be a critical factor in the evolution of disease, occurring when synapse number and transmission were already declining. This could result from increased degradation, or decreased synthesis. Prion infection in mice is known to impair the ubiquitin proteasome system, causing reduction—not increase—in protein degradation¹¹. We therefore asked if protein synthesis was reduced through translational control mechanisms. Given that total PrP levels rise during disease (Fig. 2a), and that PrP is synthesized in the endoplasmic reticulum, we examined the translational repression pathway of the unfolded protein response (UPR). Rising levels of unfolded proteins detected

¹MRC Toxicology Unit, Hodgkin Building, University of Leicester, Lancaster Road, Leicester LE1 9HN, UK. ²Centre for Analytical Bioscience, School of Pharmacy, University of Nottingham, Nottingham NG7 2RD, UK. ³MRC Laboratory of Molecular Biology, Hills Road, Cambridge CB2 0QH, UK.

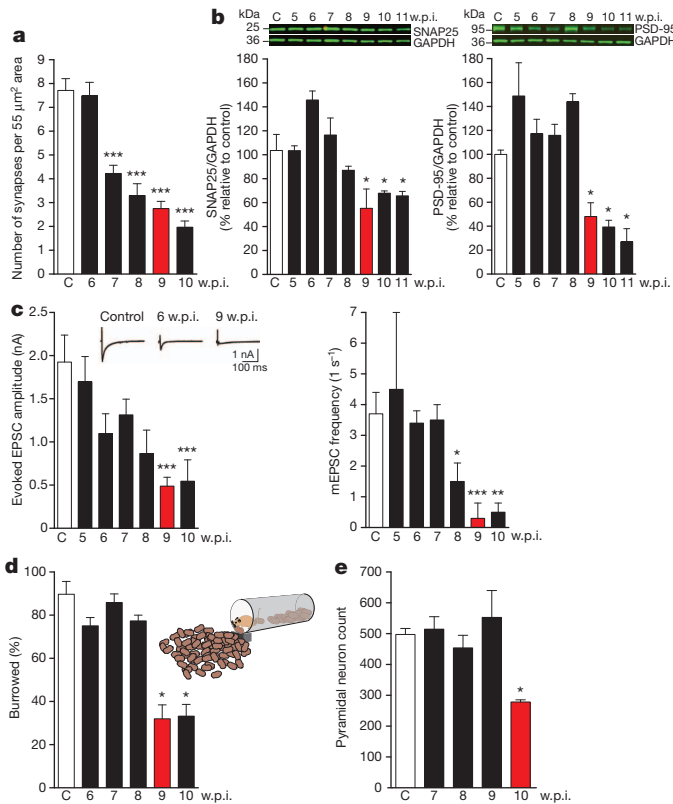


Figure 1 | Sudden decline of synaptic proteins is the key event leading to synaptic transmission failure and neuronal death in prion-diseased mice.

a, Synapse number in the stratum radiatum of the hippocampal CA1 region (imaged by electron microscopy; Supplementary Fig. 1a), declined from 7 w.p.i. ($n = 2$ mice; 32 sections per time point; $***P < 0.0001$). **b**, Levels of pre- (SNAP-25) and postsynaptic (PSD-95) proteins measured relative to GAPDH declined abruptly at 9 w.p.i. Representative western blots are shown ($n = 3$ mice per time point, $*P = 0.05$, Student's t -test; two tails). **c**, Whole-cell recordings from CA1 neurons showed significant reduction at 9 w.p.i. in both amplitude of evoked EPSCs and frequency of spontaneous mEPSCs. Representative raw traces of evoked EPSCs are shown (left panel, inset). (For **c**, $n = 2$ mice, four to eight cells per time point. $*P < 0.05$; $**P < 0.005$; $***P < 0.0001$). **d**, Burrowing behaviour declines abruptly at 9 w.p.i. ($n = 12$ mice; $**P < 0.001$, Student's t -test; two tails). **e**, Number of CA1 pyramidal neurons is reduced by approximately 50% at 10 w.p.i. ($n = 3$ mice, three sections per mouse; $*P = 0.04$). All data show mean \pm s.e.m. One-way ANOVA with Tukey's post-test was used unless otherwise stated. Control mice were injected with normal brain homogenate and examined at each time point. Data from controls at all time points was averaged, owing to lack of variability over the time course, to simplify figures. For electrophysiological recordings and electron microscopy a single control time point at 10 w.p.i. was used.

by BiP/Grp78 (BiP) in the endoplasmic reticulum membrane cause auto-phosphorylation of protein kinase-like endoplasmic reticulum kinase (PERK). PERK-P phosphorylates eIF2 α , which blocks the initiation step of translation, reducing new protein synthesis¹². eIF2 α -P then induces ATF4 and CHOP expression, ultimately leading to caspase-12 cleavage, and expression of GADD34, the stress-induced eIF2 α -P-specific phosphatase and key effector of a negative feedback loop that terminates UPR signalling, allowing translational recovery (Fig. 2g).

Upregulation of various steps in the pathway are seen in human prion cases^{13,14} and in prion-infected mice¹³; and increased phosphorylation of eIF2 α occurs in AD and PD¹⁻⁴. We characterized this pathway in prion-diseased mice. We found that PERK-P and eIF2 α -P increased throughout the course of disease (Fig. 2b, c and Supplementary Fig. 2b–d), in parallel with rising levels of total PrP, and the presence of detectable protease-resistant PrP^{Sc} (Fig. 2a). GADD34 levels did not change, despite rising eIF2 α -P levels, suggesting insufficient GADD34

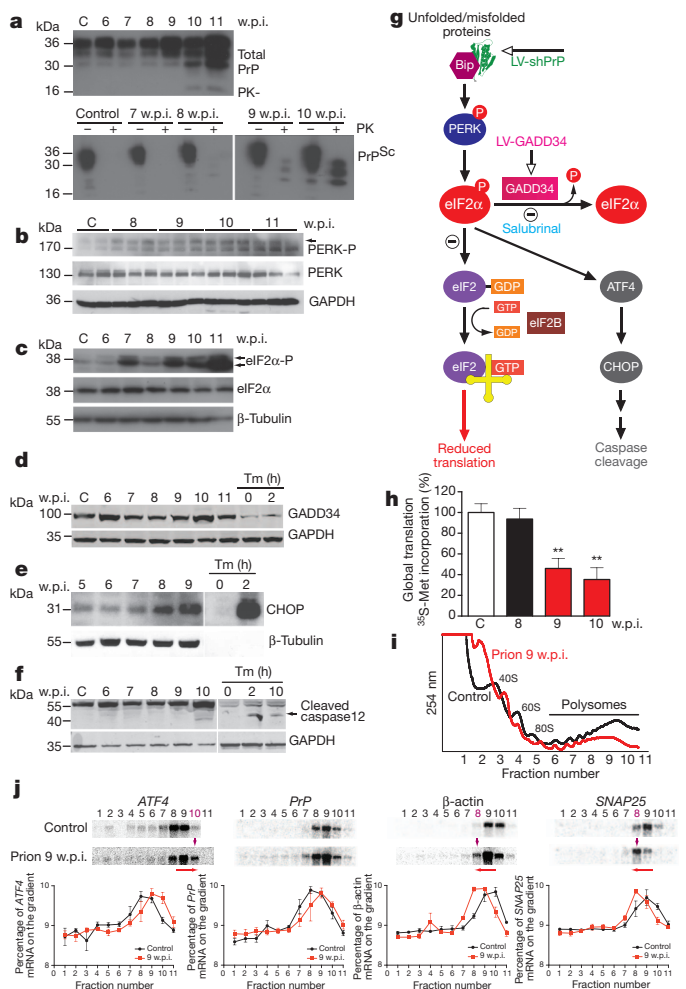


Figure 2 | Prion replication induces the UPR and results in eIF2 α -P-mediated translational repression. **a**, Total PrP and PrP^{Sc} levels (detected by addition of proteinase K (PK)) increase during prion infection; **b**, PERK-P and **c**, eIF2 α -P levels, rise during disease; **d**, GADD34 levels do not change but **e**, CHOP levels increase, throughout disease and **f**, caspase-12 is cleaved at 10 w.p.i. **g**, Scheme depicting the translational repression pathway of the UPR showing points for intervention by LV-shPrP, LV-GADD34 and salubrinal. Activation of the pathway results in reduction of global translation at 9 w.p.i. (**h**) determined by [³⁵S]methionine incorporation into hippocampal slices ($n = 3$ mice, six slices; $**P = 0.003$). **i**, Polysomal profiles from hippocampi show a reduction in active polysomes in fractions 6–11 from prion-infected mice at 9 w.p.i. **j**, Northern blots on polysomal fractions show increased translation of ATF4 with shift into fraction 10, and decreased translation of SNAP-25 and β -actin (shift into fraction 8) in prion-infected mice at 9 w.p.i. PrP translation is essentially unchanged. Quantitative line plots of northern blots show percentage of mRNA in each fraction found on the gradients. Tunicamycin (Tm)-treated HeLa cells were analysed at 0, 2 and 10 h as a control for UPR activation. All data show mean \pm s.e.m. One-way ANOVA with Tukey's post-test was used unless otherwise stated. Control mice at 11 w.p.i. are shown on western blots, and at 9 w.p.i. for northern blots and [³⁵S]methionine labelling; $n = 3$ mice for all experiments. For quantification of western blots, see Supplementary Fig. 2.

for dephosphorylation of increased eIF2 α -P (Fig. 2d and Supplementary Fig. 2e). Caspase-12 cleavage occurred at 10 w.p.i., following rising CHOP expression (Fig. 2e, f), coincident with onset of neuronal loss (Fig. 1e; see also Hetz *et al.*¹³). However, the exact effector mechanism of neuronal death is unclear: we found neither apoptosis, nor autophagy nor necrosis on examination of hippocampal slices (Supplementary Fig. 3); and neither Bax deletion, nor Bcl-2 overexpression¹⁵ nor caspase-12 deficiency¹⁶ is neuroprotective in prion disease.

We asked what effects the marked rise in eIF2 α -P levels at 9 w.p.i. had on overall protein synthesis in hippocampi. We found abrupt,

significant reduction in global translation rates, with a 50% decline in [³⁵S]methionine incorporation in hippocampal slices from prion-infected mice at 9 w.p.i. compared with mice at 8 w.p.i. and uninfected controls (Fig. 2h), confirming sudden onset of reduced protein synthesis. We also looked at translation of specific messenger RNA (mRNAs). We extracted polysomes from hippocampi of prion-infected mice. In successive polysomal fractions, mRNAs are associated with

increased numbers of actively translating ribosomes. The change from a single fraction to the next reflects a large change in translation rate for any specific mRNA. Polysomal profiles at 9 w.p.i. showed a reduction in the overall number of actively translating ribosomes, represented by the smaller area under the curve between fractions 6–11 in prion-infected mice (Fig. 2i). Northern blots for specific mRNAs in individual polysomal fractions confirmed changes in actively translated messages

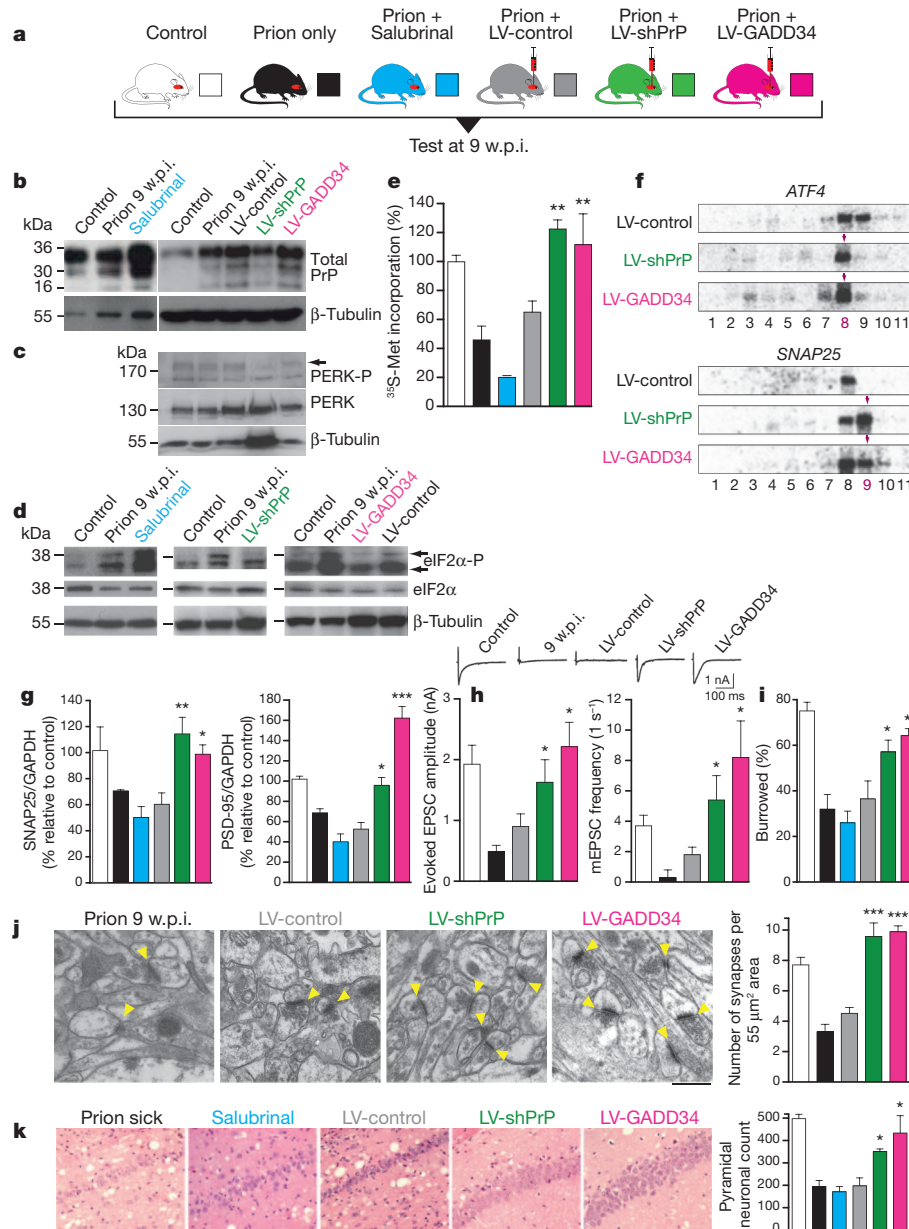


Figure 3 | Preventing eIF2 α -P formation or promoting its dephosphorylation in prion-diseased mice rescues synaptic failure and neuronal loss, while increased eIF2 α -P levels exacerbate neurotoxicity. **a**, Mice were infected with RML prions and treated with salubrinal (blue) or stereotactically injected with lentiviruses expressing anti-PrP shRNA (LV-shPrP; green), GADD34 (LV-GADD34; pink) or no insert (LV-control; grey) into both hippocampi. Control groups received no virus (prion only; black) or normal brain homogenate (control; white). Mice were tested at 9 w.p.i. **b**, LV-shPrP reduced total PrP and prevented UPR induction, reducing levels of PERK-P (**c**) and eIF2 α -P (**d**). LV-GADD34 reduced eIF2 α -P despite PERK-P induction, and salubrinal increased eIF2 α -P. **e**, Both LV-GADD34 and LV-shPrP prevented reduction in global translation at 9 w.p.i., but salubrinal reduced translation rates even further. **f**, LV-GADD34 and LV-shPrP reversed prion-induced eIF2 α -P-mediated translational changes of specific mRNAs in polysomal fractions shown on northern blots. **g**, Synaptic protein levels,

h, synaptic transmission, **i**, burrowing behaviour and **j**, synapse number were protected by GADD34 treatment and PrP knockdown. Salubrinal exacerbated protein loss. Representative electron micrographs (arrowheads denote individual synapses) and quantification are shown ($n = 2$ mice, 32 slices per mouse for each analysis). **k**, LV-GADD34 and LV-shPrP resulted in extensive neuroprotection of hippocampal CA1 pyramidal neurons and spongiosis (haematoxylin and eosin stained sections) and chart, right, when the animals were dying of scrapie at nearly 14 w.p.i. Salubrinal accelerated neurodegeneration with extensive neuronal loss seen at 9 w.p.i., earlier than in prion-sick animals at 12 w.p.i. Scale bar, 50 μ m and 2 μ m for electron micrographs. All data in bar charts show mean \pm s.e.m. One-way ANOVA with Tukey's post-test was used for multiple comparisons; * $P < 0.05$; ** $P < 0.005$; *** $P < 0.0001$. For all experiments $n = 3$ mice, unless otherwise stated. All controls were at 9 w.p.i. For quantification of Northern and western blots, see Supplementary Figs 4 and 9.

consistent with eIF2 α -P induction. Thus *SNAP-25* and β -*actin* mRNAs showed a left shift to a lower polysomal fraction (Fig. 2j), representing reduced active translation (Fig. 1b). In contrast, *ATF4* mRNA (which escapes eIF2 α -P-mediated inhibition of translation, owing to the presence of upstream open reading frames in its 5' untranslated region (UTR)^{17,18}), showed increased active translation, represented by a right shift to a higher polysomal fraction (Fig. 2j and Supplementary Figs 4 and 5). *PrP* mRNA did not show reduced translation, possibly because of the existence of similar translational control elements within the *PrP* gene. Indeed, human *PrP* mRNA has multiple upstream AUG upstream open reading frames in its 5' UTR, which could allow it to escape eIF2 α -P translational inhibition in the same way as *ATF4* does^{17,18} (Supplementary Fig. 6).

Overall, these findings confirm that reduction in protein synthesis in prion disease is controlled at the translational, not the transcriptional, level, as it is rates of translation, not levels of total mRNA, that change (Supplementary Figs 1c and 2g, h).

We propose that the key trigger to prion neurodegeneration is the continued, unchecked activation of the UPR due to rising levels of PrP during disease, with fatal repression of translation rates. Importantly, prion neurotoxicity relates in a dose-dependent manner to PrP expression^{19–21}. We therefore asked if levels of eIF2 α -P and onset of neurodegeneration were related to levels of PrP in different strains of mice. We found that in homozygous tg37 mice, which overexpress PrP approximately sixfold, eIF2 α -P was induced at 6 w.p.i., and mice succumbed to prion infection at approximately 8 w.p.i. In wild-type C57/Bl6 mice, which express 1 \times levels of PrP, eIF2 α -P was induced at 16 w.p.i. and animals succumbed at approximately 22 w.p.i. Thus, as for hemizygous tg37 mice where PrP was expressed at three times wild-type levels and eIF2 α -P was induced at 9 w.p.i. followed by death at 12 w.p.i. (Fig. 2c), in each case there was a corresponding critical decline in synaptic proteins and synapse number after eIF2 α -P induction (Supplementary Fig. 7 and Fig. 1a, b).

Transient eIF2 α phosphorylation is beneficial to cells overloaded with misfolded proteins: it reduces protein synthesis and increases availability of chaperones, promoting refolding^{22,23}. However, persistently high levels of eIF2 α -P are detrimental *in vitro*²⁴. To test directly the role of eIF2 α -P in prion neurodegeneration *in vivo*, we first asked if reduction of eIF2 α -P levels in prion disease would be neuroprotective. We used two approaches. We overexpressed GADD34, the eIF2 α -P-specific phosphatase to reduce eIF2 α -P levels directly. In a separate experiment, we used targeted RNA interference of PrP to abrogate UPR activation and prevent eIF2 α -P formation. We then asked if increased levels of eIF2 α -P exacerbate prion neurotoxicity by using salubrinal, a specific small-molecule inhibitor of eIF2 α -P dephosphorylation⁵, in infected mice. Salubrinal penetrates the blood–brain barrier (Supplementary Fig. 8) and has been used for modulation of eIF2 α -P-dependent effects in endoplasmic reticulum stress-mediated processes in the central nervous system *in vivo* after peripheral administration^{25–27}. Mice were inoculated with prions and received hippocampal injections of lentiviruses expressing GADD34 (LV-GADD34), anti-PrP shRNA (LV-shPrP) or yellow fluorescent protein (YFP) only (LV-control) at 5 w.p.i., allowing 4 weeks for lentiviral expression to occur, before testing the effects of treatment on eIF2 α -P levels and neurotoxicity at 9 w.p.i. (All virally expressed constructs were driven by the CAMKII promoter for neuron-specific expression (Supplementary Fig. 9a–c)). Another group of prion-infected mice received daily intraperitoneal injections of salubrinal (1 mg kg⁻¹), for 1 week, from 8 w.p.i., with controls receiving vehicle alone. Two further control groups received normal brain homogenate, or RML prion inoculation alone (Fig. 3a).

We examined mice from each group at 9 w.p.i. when eIF2 α -P-mediated translational repression occurs (Fig. 2c, h). LV-GADD34 treatment did not reduce PrP levels (Fig. 3b) and PERK-P levels were equivalent to those in prion-only or LV-control treated animals (Fig. 3c and Supplementary Fig. 9d), confirming UPR activation in

these mice. Critically, however, eIF2 α -P levels were reduced (Fig. 3d and Supplementary Fig. 9e), strongly supporting its dephosphorylation by lentivirally mediated GADD34 expression. LV-shPrP treatment reduced PrP levels (Fig. 3b) and prevented the PrP-induced rise in PERK-P and eIF2 α -P seen in untreated animals (Fig. 3c, d), confirming prevention of UPR activation. Both GADD34 overexpression and PrP knockdown prevented prion-induced eIF2 α -P-mediated translational repression, with restoration of global rates at 9 w.p.i. (Fig. 3e) and prevention of eIF2 α -P-induced changes in translation of specific mRNAs (Fig. 3f and Supplementary Fig. 4). As a result, synaptic protein levels, synaptic transmission and synapse number in prion-diseased mice treated with GADD34 or PrP knockdown were protected and equivalent to levels in uninfected control mice (Fig. 3g, h, j). Burrowing deficits were prevented (Fig. 3i) and there was extensive neuronal protection in the hippocampus, with no neuronal loss and markedly reduced spongiform change (Fig. 3k). Further, targeted expression of LV-GADD34 and focal PrP knockdown had a modest, but highly significant, effect on survival, increasing this to 90 \pm 3 days and 92 \pm 5 days respectively, compared with 83 \pm 2 days for prion-only mice (Fig. 4), and to 82 \pm 2 days for LV-control injected mice (Supplementary Fig. 10). For both LV-GADD34 and LV-shPrP, treatment was localized to the dorsal hippocampus, a very small area of the brain, so prion infection in the rest of the brain was fatal, but neuroprotection in GADD34-treated animals was seen even when the animals were terminally sick (Fig. 3k). More extensive brain-wide delivery of GADD34, or targeting of this pathway, would be predicted to increase survival further and give more widespread neuroprotection. Critically, treatment with salubrinal had the opposite effect, by preventing dephosphorylation of eIF2 α -P. Thus, eIF2 α -P levels were markedly higher at 9 w.p.i. than in prion-only controls (Fig. 3d and Supplementary Fig. 9e), causing further repression of global translation (Fig. 3e) and reduction of synaptic proteins (Fig. 3g). Salubrinal treatment resulted in earlier severe neuronal loss (Fig. 3k), and significantly accelerated disease, compared with untreated prion-infected mice (Fig. 4).

In conclusion, we have shown that PrP replication causes sustained UPR induction with persistent, deleterious expression of eIF2 α -P in prion disease. The resulting chronic blockade of protein synthesis leads to synaptic failure, spongiosis and neuronal loss. Promoting eIF2 α -P dephosphorylation rescues vital translation rates and is thereby neuroprotective, whereas preventing this further reduces translation and enhances neurotoxicity. The data support the development of generic proteostatic approaches^{22,28} to therapy—fine-tuning protein synthesis—in prion, and perhaps other neurodegenerative disorders involving protein misfolding.

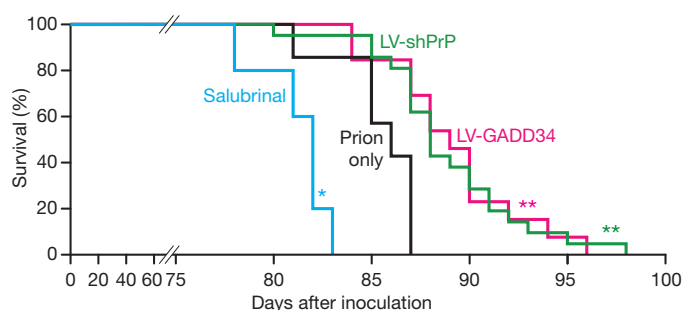


Figure 4 | Reducing eIF2 α -P levels in prion-diseased mice significantly increases survival. Kaplan–Meier survival plots for prion-infected mice treated with salubrinal ($n = 10$), prions alone ($n = 7$), hippocampal injections of LV-GADD34 ($n = 13$) or LV-shPrP ($n = 14$). Focal treatment with LV-GADD34 and LV-shPrP resulted in significantly increased survival compared with prion-infected mice with no treatment (** $P = 0.007$; Student's *t*-test); salubrinal treatment reduced survival (* $P = 0.03$). For plots for LV-control and DMSO controls, see Supplementary Fig. 10.

METHODS SUMMARY

Prion infection of mice. All animal work conformed to UK regulations and institutional guidelines, performed under Home Office guidelines. tg37 (ref. 10) and C57/Bl6N mice (Harlan) were inoculated with 1% brain homogenate of Chandler/RML prions aged 3–4 weeks, as described⁷. Animals were culled when they developed clinical signs of scrapie. Control mice received 1% normal brain homogenate. Hippocampi were processed for protein, RNA or histological analysis^{7–10}. For all analyses $n = 3$ mice unless otherwise stated.

Lentiviruses and stereotaxic surgery. Lentiviral plasmids were generated using the Invitrogen Gateway cloning system²⁹. The neuron-specific promoter CAMKII was used to drive shPrP expression, carboxy (C)-terminal GADD34 expression, or YFP alone (control virus). Viruses were injected stereotaxically into the CA1 region of the hippocampus as described⁹.

Salubrial treatment. Mice received daily intraperitoneal injections of 1 mg kg⁻¹ of salubrial (Calbiochem), or vehicle (diluted dimethylsulphoxide (DMSO) in saline (Sigma))²⁵, for 7 days from 8 w.p.i.

Experimental analyses. Synapse numbers were counted in electron micrographs of the stratum radiatum of the hippocampal CA1 region³⁰. Synaptic marker proteins, UPR pathway proteins and PrP were analysed by immunoblotting of brain homogenates. PrP^{Sc} was detected after proteinase K digestion⁷. Whole-cell recordings were done in acute hippocampal slices to measure synaptic transmission³¹. Global translation levels were detected using [³⁵S]methionine incorporation in acute hippocampal slices; translations of specific transcripts in polysomal fractions from hippocampi were analysed by northern blotting³². Neuronal counts were determined by quantifying NeuN-positive pyramidal CA1 neurons⁹. All analyses were performed using hippocampi from three mice in triplicate unless otherwise stated. Burrowing behaviour was performed as described on groups of 10 or more mice⁸. Statistical analyses were performed using GraphPad/Prism software, version 5, using Student's *t*-test for data sets with normal distribution and a single intervention. Analysis of variance (ANOVA) testing was performed using one-way analysis with Tukey's post-hoc test for multiple comparisons.

Full Methods and any associated references are available in the online version of the paper at www.nature.com/nature.

Received 11 October 2011; accepted 16 March 2012.

Published online 6 May 2012.

- Hoozemans, J. J. *et al.* Activation of the unfolded protein response in Parkinson's disease. *Biochem. Biophys. Res. Commun.* **354**, 707–711 (2007).
- Hoozemans, J. J. *et al.* The unfolded protein response is activated in pretangle neurons in Alzheimer's disease hippocampus. *Am. J. Pathol.* **174**, 1241–1251 (2009).
- Hoozemans, J. J. *et al.* The unfolded protein response is activated in Alzheimer's disease. *Acta Neuropathol.* **110**, 165–172 (2005).
- Unterberger, U. *et al.* Endoplasmic reticulum stress features are prominent in Alzheimer disease but not in prion diseases *in vivo*. *J. Neuropathol. Exp. Neurol.* **65**, 348–357 (2006).
- Boyce, M. *et al.* A selective inhibitor of eIF2 α dephosphorylation protects cells from ER stress. *Science* **307**, 935–939 (2005).
- Prusiner, S. B. Molecular biology of prion diseases. *Science* **252**, 1515–1522 (1991).
- Mallucci, G. *et al.* Depleting neuronal PrP in prion infection prevents disease and reverses spongiosis. *Science* **302**, 871–874 (2003).
- Mallucci, G. R. *et al.* Targeting cellular prion protein reverses early cognitive deficits and neurophysiological dysfunction in prion-infected mice. *Neuron* **53**, 325–335 (2007).
- White, M. D. *et al.* Single treatment with RNAi against prion protein rescues early neuronal dysfunction and prolongs survival in mice with prion disease. *Proc. Natl Acad. Sci. USA* **105**, 10238–10243 (2008).
- Mallucci, G. R. *et al.* Post-natal knockout of prion protein alters hippocampal CA1 properties, but does not result in neurodegeneration. *EMBO J.* **21**, 202–210 (2002).
- Kristiansen, M. *et al.* Disease-associated prion protein oligomers inhibit the 26S proteasome. *Mol. Cell* **26**, 175–188 (2007).
- Ron, D. & Walter, P. Signal integration in the endoplasmic reticulum unfolded protein response. *Nature Rev. Mol. Cell Biol.* **8**, 519–529 (2007).
- Hetz, C., Russelakis-Carneiro, M., Maundrell, K., Castilla, J. & Soto, C. Caspase-12 and endoplasmic reticulum stress mediate neurotoxicity of pathological prion protein. *EMBO J.* **22**, 5435–5445 (2003).
- Yoo, B. C. *et al.* Overexpressed protein disulfide isomerase in brains of patients with sporadic Creutzfeldt-Jakob disease. *Neurosci. Lett.* **334**, 196–200 (2002).
- Steele, A. D. *et al.* Diminishing apoptosis by deletion of Bax or overexpression of Bcl-2 does not protect against infectious prion toxicity *in vivo*. *J. Neurosci.* **27**, 13022–13027 (2007).
- Steele, A. D. *et al.* Prion pathogenesis is independent of caspase-12. *Prion* **1**, 243–247 (2007).
- Harding, H. P. *et al.* Regulated translation initiation controls stress-induced gene expression in mammalian cells. *Mol. Cell* **6**, 1099–1108 (2000).
- Spriggs, K. A., Bushell, M. & Willis, A. E. Translational regulation of gene expression during conditions of cell stress. *Mol. Cell* **40**, 228–237 (2010).
- Bueler, H. *et al.* Mice devoid of PrP are resistant to scrapie. *Cell* **73**, 1339–1347 (1993).
- Manson, J. C., Clarke, A. R., McBride, P. A., McConnell, I. & Hope, J. PrP gene dosage determines the timing but not the final intensity or distribution of lesions in scrapie pathology. *Neurodegeneration* **3**, 331–340 (1994).
- Sandberg, M. K., Al-Doujaily, H., Sharps, B., Clarke, A. R. & Collinge, J. Prion propagation and toxicity *in vivo* occur in two distinct mechanistic phases. *Nature* **470**, 540–542 (2011).
- Tsaytler, P., Harding, H. P., Ron, D. & Bertolotti, A. Selective inhibition of a regulatory subunit of protein phosphatase 1 restores proteostasis. *Science* **332**, 91–94 (2011).
- Chafekar, S. M., Hoozemans, J. J., Zwart, R., Baas, F. & Scheper, W. A β _{1–42} induces mild endoplasmic reticulum stress in an aggregation state-dependent manner. *Antioxid. Redox Signal.* **9**, 2245–2254 (2007).
- Wiseman, R. L. *et al.* Flavonol activation defines an unanticipated ligand-binding site in the kinase-RNase domain of IRE1. *Mol. Cell* **38**, 291–304 (2010).
- Sokka, A. L. *et al.* Endoplasmic reticulum stress inhibition protects against excitotoxic neuronal injury in the rat brain. *J. Neurosci.* **27**, 901–908 (2007).
- Saxena, S., Cabuy, E. & Caroni, P. A role for motoneuron subtype-selective ER stress in disease manifestations of FALS mice. *Nature Neurosci.* **12**, 627–636 (2009).
- Zhu, Y. *et al.* Eif-2a protects brainstem motoneurons in a murine model of sleep apnea. *J. Neurosci.* **28**, 2168–2178 (2008).
- Balch, W. E., Morimoto, R. I., Dillin, A. & Kelly, J. W. Adapting proteostasis for disease intervention. *Science* **319**, 916–919 (2008).
- White, M. D., Milne, R. V. & Nolan, M. F. A molecular toolbox for rapid generation of viral vectors to up- or down-regulate neuronal gene expression *in vivo*. *Front. Mol. Neurosci.* **4**, 8 (2011).
- Haustein, M. D. *et al.* Acute hyperbilirubinaemia induces presynaptic neurodegeneration at a central glutamatergic synapse. *J. Physiol. (Lond.)* **588**, 4683–4693 (2011).
- Steinert, J. R. *et al.* Nitric oxide is an activity-dependent regulator of target neuron intrinsic excitability. *Neuron* **71**, 291–305 (2011).
- Johannes, G. & Sarnow, P. Cap-independent polysomal association of natural mRNAs encoding c-myc, BiP, and eIF4G conferred by internal ribosome entry sites. *RNA* **4**, 1500–1513 (1998).

Supplementary Information is linked to the online version of the paper at www.nature.com/nature.

Acknowledgements We thank D. Read for imaging analysis, J. Edwards, T. Smith, J. McWilliam, P. Glynn, C. Molloy and University of Leicester, Department of Biological Services staff for technical assistance, J. Collinge (MRC Prion Unit) for the original RML prion inoculum, and K. Little for reading the manuscript. This work was funded by the Medical Research Council, UK.

Author Contributions J.A.M. did most of the experimental work and analysis. N.V. and M.G.M. performed stereotaxic surgery and prion inoculations. H.R., D.P., M.H. and J.M. performed various experiments, D.D. performed electron microscopy, J.R.S. performed electrophysiological analysis, C.A.O. and D.A.B. performed mass spectrometry analysis, P.T. and A.B. worked with J.A.M. in Cambridge, A.E.W. and M.B. contributed expertise and direction on translational control mechanisms, and G.R.M. directed and supervised the project. J.A.M. and G.R.M. wrote the paper. All authors contributed to discussion, analysis of data and the final draft of paper.

Author Information Reprints and permissions information is available at www.nature.com/reprints. The authors declare no competing financial interests. Readers are welcome to comment on the online version of this article at www.nature.com/nature. Correspondence and requests for materials should be addressed to G.R.M. (grm7@le.ac.uk).

METHODS

Prion infection of mice. All animal work conformed to UK regulations and institutional guidelines, performed under Home Office guidelines. tg37 (ref. 10) and C57/Bl6N mice (Harlan) were inoculated with 1% brain homogenate of Chandler/RML prions aged 3–4 weeks, as described⁷. Animals were culled when they developed clinical signs of scrapie. Control mice received 1% normal brain homogenate. Hippocampi were processed for protein, RNA or histological analysis^{7–10}. For all analyses $n = 3$ mice unless otherwise stated.

Lentiviruses and stereotaxic surgery. Lentiviral plasmids were generated using the Invitrogen Gateway cloning system²⁹. The neuron-specific promoter CAMKII was used to drive shPrP expression, C-terminal GADD34 expression, or YFP alone (control virus). Viruses were injected stereotaxically into the CA1 region of the hippocampus as described⁹.

Salubral treatment. Mice received daily intraperitoneal injections of 1 mg kg⁻¹ of salubrinal (Calbiochem), or vehicle (diluted DMSO in saline (Sigma))²⁵, for 7 days from 8 w.p.i.

Experimental analyses. Synapse numbers were counted in electron micrographs of the stratum radiatum of the hippocampal CA1 region³⁰. Synaptic marker proteins, UPR pathway proteins and PrP were analysed by immunoblotting of brain homogenates. PrP^{Sc} was detected after proteinase K digestion⁷. Whole-cell recordings were done in acute hippocampal slices to measure synaptic transmission³¹. Global translation levels were detected using [³⁵S]methionine incorporation in acute hippocampal slices; translations of specific transcripts in polysomal fractions from hippocampi were analysed by northern blotting³². Neuronal counts were determined by quantifying NeuN-positive pyramidal CA1 neurons⁹. All analyses were performed using hippocampi from three mice in triplicate unless otherwise stated. Burrowing behaviour was performed as described on groups of 10 or more mice⁸. Statistical analyses were performed using GraphPad/Prism software, version 5, using Student's *t*-test for data sets with normal distribution and a single intervention. ANOVA testing was performed using one-way analysis with Tukey's post-hoc test for multiple comparisons.

Generation of lentiviral plasmids. Lentiviral plasmids were generated by using the Invitrogen Gateway cloning system as described²⁹. ATT-flanked cassettes were constructed by PCR amplification using ATT recombination site sequences and 20–25 template-specific sequences. The C terminus GADD34 cassette was amplified from Flag-tagged C-term GADD34 using attB5 5'-GGGGACAACCTTTGTATACAAAAGTTGGCCACCATGCGTTCAGGAGAGGCGTCCGA-3'; and attB4 5'-GGGGACAACCTTTGTATAGAAAAGTTGGGTGTTGGTCTCAGCCACGCCTCCAC-3' primers; WPRE and YFP cassettes were amplified from pLL3.7-shPrP plasmid using attB3 5'-GGGGACAACCTTTGTATAATAAAGTTGTCACCTCTGGATTACAAAATTTGT-3' and attB2 5'-GGGGACCACTTTGTACAAGAAAGCTGGGTATGCGGGAGGCGGCCCAAAGGGAGA-3' primers for WPRE and attB4r 5'-ACCATGGTGAGCAAGGGCGA-3' and attB3r 5'-TTACTTGTACAGCTCGTCCATGCCG-3' primers for YFP. The CAMKII promoter was amplified from mouse cDNA using attB1 5'-GGGGACAA GTTTGTACAAAAGCAGGCTACTTGTGGACTAAGTTTGTTCGC-3' and attB5r primer 5'-GGGGACAACCTTTGTATACAAAAGTTGTCTGCCCCAGACTAGGG-3' primers. Cassettes were amplified and recombined into appropriate pDONR entry vectors. Once the entry plasmids were generated they were recombined with the pLenti6/BLOCK-IT/DEST vector (Invitrogen) to construct lentiviral plasmids. We used lentiviral plasmids containing shPrP and empty vector constructs as described⁹. Lentiviruses were generated using DNA/Ca²⁺ phosphate transfection of HEK293 cells³³. Additional stocks of virus were generated by GenTarget and titre determined using fluorescence-activated cell sorting (BD FACS Calibur). Viruses were used with a final titre of 0.6×10^8 to 1.5×10^8 TU.

Stereotaxic injection. Mice were anaesthetized using isoflurane. Injections were into the CA1 region of the hippocampus as described⁹.

Electron microscopy. Semi-thin sections for electron microscopy were obtained by terminal perfusion of mice as described³⁰. Ultrathin sections (70 nm) were examined in a JEOL 100-CXII electron microscope (JEOL (UK) equipped with a 'Megaview III' digital camera (Olympus Soft Imaging Solutions). Synapses were scored using criteria of structures showing a postsynaptic density, containing synaptic vesicles and a synaptic junction. Thirty-two images from two mice were used for scoring.

Electrophysiology. Whole-cell recordings were made from identified CA1 neurons and recording performed as described³⁰. In brief, neurons were voltage clamped

using a Multiclamp 700B amplifier and pClamp 10.3 software (Molecular Devices) and EPSCs were evoked by stimulation with bipolar platinum electrode at 37 °C. Pipettes (2.5–3.5 M Ω) were filled with a solution containing (in mM): KCl 110, HEPES 40, EGTA 0.2, MgCl₂ 1, CaCl₂ 0.1; pH was adjusted to 7.2 with KOH. Neurons were visualized with $\times 60$ objective lenses on a Nikon FS600 microscope fitted with differential interference contrast optics. Four to eight cells were measured per mouse in at least two animals per experiment.

Immunoblotting. Protein samples were isolated from hippocampi using protein lysis buffer (50 mM Tris, 150 mM NaCl, 2 mM EDTA, 1 mM MgCl₂, 100 mM NaF, 10% glycerol, 1% Triton X-100, 1% Na deoxycholate, 0.1% SDS and 125 mM sucrose) supplemented with Phos-STOP and protease inhibitors (Roche). Synaptic protein levels were determined by resolving 20 mg of protein on SDS-polyacrylamide gel electrophoresis gels, transferred onto nitrocellulose membrane and incubated with primary antibodies, SNAP-25, (1:10,000; Abcam), VAMP2 (1:5,000; Synaptic Systems), NMDA-R1 (1:1,000; Sigma) and PSD95 (1:1,000; Millipore). Odyssey IRDye800 secondary antibodies (1:5,000; LI-COR) were applied, visualized and quantified using Odyssey infrared imager (LI-COR; software version 3.0). Protein for PrP levels and UPR pathway activation were determined using the primary antibodies, 8H4 for total PrP (1:1,000; Abcam), ICSM35 for PrP^{Sc} (1:10,000; D-GEN), PERK-P, total PERK, P-eIF2 α , eIF2 α (1:1,000; Cell Signaling), CHOP (1:1,000; ThermoScientific), caspase-12 (1:1,000; Exalpha), BiP/Grp78 (1:1,000; Stressgen) and GADD34 (1:1,000; ProteinTech). Horseradish-peroxidase-conjugated secondary antibodies (1:5,000; DAKO) were applied and protein visualized using enhanced chemiluminescence (GE Healthcare) and quantified using ImageJ. Antibodies against GAPDH (1:5,000; Santa Cruz) or β -tubulin (1:5,000; Millipore) were used to determine loading.

Hippocampal slice preparation and [³⁵S]methionine labelling. Slices were dissected in an oxygenated cold (2–5 °C) sucrose artificial cerebrospinal fluid containing (in mM): 26 NaHCO₃, 2.5 KCl, 4 MgCl₂, 0.1 CaCl₂, and 250 sucrose. Hippocampal slices were prepared using a tissue chopper (McIlwain). Slices were allowed to recover in normal artificial cerebrospinal fluid buffer while being oxygenated at 37 °C for 1 h, incubated with [³⁵S] methionine label for 1 h, then homogenized. Proteins were precipitated with trichloroacetic acid; incorporation of radiolabel was measured by scintillation counting (Winspectral, Wallac).

Polysomal fraction preparation and northern blots. Sucrose density gradient centrifugation was used to separate hippocampal homogenates into polysomal and subpolysomal fractions. Polysomal fractions were isolated as described³². Briefly, hippocampi were dissected in ice-cold gradient buffer (0.3 M NaCl, 15 mM MgCl₂, 15 mM Tris-HCl (pH 7.4), 0.1 mg ml⁻¹ cyclohexamide and 1 mg ml⁻¹ heparin). The hippocampal tissue was homogenized in gradient buffer containing RNase inhibitors and 1.2% TritonX-100 added. Samples were centrifuged and the supernatants layered onto 10–60% sucrose gradients. The gradients were sedimented at 38,000 r.p.m. using a TH-641 rotor (Thermo Scientific) for 120 min at 4 °C. One millilitre fractions were collected from the gradients into 3 ml of 7.7 M guanidine-HCl using a Foxy R1 gradient fractionator (Teledyne ISCO; ISCO peak Trak version 1.10 software) with continuous measurement of the absorbance at 254 nm. RNA was then isolated and equal volumes of each fraction were analysed by northern blot analysis³².

Neuropathological examination of brain sections. Paraffin-embedded brains were either stained with haematoxylin and eosin (H&E) or incubated with NeuN antibody (1:200; Millipore) for neuronal counts. CA1 pyramidal neuron counts were determined using three serial sections from three separate mice. All images were taken using a Zeiss Axiovert 200M microscope with a Colibri illumination system with Axiovision 4.8 software (Zeiss) and NeuN positive cells were counted using the Velocity v.5 (Perkin Elmer) software.

Burrowing. Burrowing was performed as described. At least 10 mice were burrowed for each individual experimental group^{10,34}.

Statistical analysis. Student's *t*-tests were applied to all data sets with two tails (two samples; unequal variance). ANOVA testing was performed using one-way analysis with Tukey's post-hoc test for group effects. Statistical tests were performed using GraphPad/Prism version 5. All data in bar charts show mean \pm s.e.m.

- Jiang, M., Deng, L. & Chen, G. High Ca²⁺-phosphate transfection efficiency enables single neuron gene analysis. *Gene Ther.* **11**, 1303–1311 (2004).
- Cunningham, C. *et al.* Synaptic changes characterize early behavioural signs in the ME7 model of murine prion disease. *Eur. J. Neurosci.* **17**, 2147–2155 (2003).